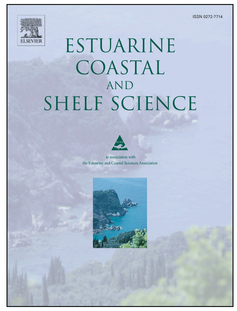

Variability of depth-limited waves in coral reef surf zones

Daniel L. Harris, Hannah E. Power, Michael A. Kinsela, Jody M. Webster, Ana Vila-Concejo

PII: S0272-7714(16)30798-3

DOI: 10.1016/j.ecss.2018.06.010

Reference: YECSS 5886

To appear in: *Estuarine, Coastal and Shelf Science*

Received Date: 30 December 2016

Revised Date: 5 June 2018

Accepted Date: 11 June 2018

Variability of depth-limited waves in coral reef surf zones

Daniel L. Harris[1,2,3*], Hannah E. Power[4], Michael A. Kinsela[5], Jody M. Webster[6] and Ana Vila-Concejo[6]

[1] School of Earth and Environmental Sciences, The University of Queensland, Brisbane, QLD, 4072, Australia

[2] Leibniz Center for Tropical Marine Research (ZMT), Bremen, Germany

[3] Center for Marine Environmental Sciences (MARUM), The University of Bremen, Bremen, Germany

[4] School of Environmental and Life Sciences, The University of Newcastle, Callaghan, Australia

[5] Coastal and Marine Unit, NSW Office of Environment and Heritage, Sydney, NSW 2000, Australia

[6] Geocoastal Research Group, School of Geosciences, The University of Sydney, NSW, 2006, Australia

[*]corresponding author daniel.harris@uq.edu.au

Abstract

Wave breaking and transformation on coral reef flats is an important process protecting tropical coastlines and regulating the energy regimes of coral reefs. However, the high hydraulic roughness, shallow water, and steep bathymetries of coral reefs may confound common surf zone assumptions, such as a depth-limited and saturated surf zone with a constant wave height to water depth ratio (γ). Here, we examine wave transformation across a coral reef flat, during three separate swell events, on both a time-averaged and a wave-by-wave basis. We use the relationship between significant wave height and water depth (γ_s) to examine the change in surf saturation across the reef flat and compare the measured wave height decay to results of modelled wave energy dissipation in the surf zone. Our results show that γ_s was not cross-reef constant and varied according to location on the reef flat and local water depth. On average, γ_s was greatest at the outer reef flat, near the reef crest, and progressively reduced towards the inner reef flat, near the reef lagoon. This was most pronounced in shallow water with large γ_s values ($\gamma_s > 0.85$) at the outer reef flat and small γ_s values ($\gamma_s < 0.1$) at the inner reef flat. This indicates that there is an increase in wave energy dissipation in shallow water, most likely due to increased breaker and bed frictional dissipation. The measured wave energy dissipation across the entire reef flat could, on average, be modelled accurately; however, this required location specific calibration of the free parameters, the wave friction factor (f_w) and γ, and further suggests that there is no value for either parameter that is universally applicable to coral reef flats. Despite model calibration inaccuracies were still observed, primarily at the outer reef flat. These inaccuracies reflected the observed cross-reef variation of γ on the reef flat and potentially the limitations of random wave breaker dissipation models in complex surf zones. Our results have implications for the use of wave energy dissipation models in predicting breaker dissipation and subsequent benthic community change on coral reef flats, and

suggest that careful consideration of the free parameters in such models (such as f_w and γ) is required.

Introduction

Coastal protection and the regulation of hydrodynamic energy is one of the most important ecosystem services provided by coral reef systems (e.g. Hoegh-Guldberg et al., 2007). Wave breaking and transformation on coral reef flats, and the resultant wave induced flows, are the dominant physical forcing mechanisms on most coral reefs (Monismith, 2007). The shallow water environment and very high frictional roughness values of reef flats contribute to the efficient removal of wave energy over relatively short distances (Lowe et al., 2005; Monismith et al., 2015). As a result of this process, back-reef environments immediately in lee of coral reef flats are typically low-energy environments with limited potential for sediment transport under average conditions (Harris et al., 2015; Pomeroy et al., 2012).

Wave energy dissipation in the surf zone of coral reefs is similar to beach environments in that it has mostly been observed to saturate (Gourlay, 1994; Nelson, 1994), with a constant ratio of wave height (H) to water depth (h) over time:

$$H = \gamma h \quad \text{(Eq. 1)}$$

where γ is the wave height to water depth ratio . For saturated surf zones the common values used for γ are: 0.78 for monochromatic waves, which was first derived from solitary wave theory and observed in laboratory studies (Longuet-Higgins, 1974; McCowan, 1891); and, 0.42 for root-mean square wave height (H_{rms}) which was observed in surf zones of beaches (e.g. Sallenger and Holman, 1985; Thornton and Guza, 1982). However, these values were derived from a limited range of conditions and beach types, and a wide range of γ has been observed in more complex beach environments including observations of nonconstant γ in the cross-shore in unsaturated surf (Nelson, 1987; Power et al., 2010; Raubenheimer et al., 1996; Ruessink et al., 2003).

Coral reefs have been the subject of even fewer surf-zone studies compared to siliciclastic beaches and typically have much more complex bathymetries (Demirbilek and Nwogu, 2007). As a result γ may be poorly defined for coral reefs, despite γ being the primary parameter that defines wave breaking in many wave energy dissipation models (e.g. Baldock et al., 1998; Battjes and Janssen, 1978; Thornton and Guza, 1983). These models and concepts have been applied to coral reefs to infer changes in coral reef geomorphology and ecology (Gove et al., 2015), and to determine the coastal protection service provided by coral reefs (Harris et al., 2018; Saunders et al., 2014; Storlazzi et al., 2015). They have also been used to link hydraulic roughness observations to benthic ecological assemblages and to determine the influence of waves on ecological zonation of coral reefs (Monismith et al., 2015; Rogers et al., 2016; Storlazzi et al., 2005; Williams et al., 2013). Most of these analyses are reliant on an accurate description of breaker wave energy dissipation on coral reef flats despite the limited data in such systems when compared to siliciclastic beaches. This study will therefore focus on wave transformation and the variationn of surf zone saturation and depth limited waves across the reef flat and determine what influence this may have on the accuracy on breaker dissipation models.

The most common value of γ observed on coral reef flats is between $\gamma = 0.4 – 0.6$, which has been observed in both laboratory and field studies (Table S1). However, this value is mostly applicable only to the near-horizontal reef flats and may not be relevant for the steep fore-reef slopes of coral reefs (Massel and Gourlay, 2000; Nelson, 1994). When the full cross-reef profile is examined (including the fore-reef slope and the reef crest) a wide range of γ values have been observed ($0.1 < \gamma < 1.2$) (Figure 1 and Table S1). This may be due to one or a combination of: 1) the many different definitions of γ that have been reported; 2) the numerous methods used to determine γ; and/or, 3) the location of observation on the reef flat (Figure 1 and Table S1). Cross-reef variability in γ has been previously observed with γ values between 0.7 – 1.2 for the fore-reef slope and reef crest, and 0.2 – 0.7 for the reef flat (Figure 1 and Table S1).

The observed variability of γ values across the surf zones of coral reefs has led to concerns regarding the accuracy of commonly used wave energy dissipation models that use a constant value of γ to determine the proportion of broken waves, for a given period, in the surf zone (Demirbilek and Nwogu, 2007). In an attempt to mitigate this, Hearn (1999) incorporated the observed cross-reef variability of γ into models of wave energy dissipation and defined regions of high γ (at the reef crest, $\gamma = 0.8$) and low γ (on the reef flat, $\gamma = 0.5$). These values are similar to the average results found in previous literature, when examining γ values with respect to the location on the reef flat (Figure 1). However, most wave energy dissipation models, including the most common models that have been used on coral reefs, use a constant γ parameter to define wave breaker dissipation (e.g. Harris et al., 2018; Lowe et al., 2005; Pomeroy et al., 2012). In these scenarios, wave energy dissipation models have primarily been calibrated to describe the total dissipation of energy across the coral reef flats and, while accurately explaining wave energy dissipation in general terms, they may overlook some specific wave processes and conditions that differ between the outer reef (near or at break point) and the inner reef flats (inner surf zone) (Massel and Gourlay, 2000). Furthermore, the common approach of using time-averaged measurement and modelling of coral reef surf zone processes may mask significant detail in the true variation of wave heights in the inner surf zone. Previous studies have found that individual waves in surf zones of intermediate beaches are not necessarily influenced by water depth to the same extent as time-averaged wave conditions (e.g. Power et al., 2010; Power et al., 2015). To date there has been no detailed wave-by-wave analysis of measured wave transformation in a coral reef surf zone. Therefore, this study will: 1) examine the variability and prevalence of surf zone saturation and depth limited waves by analysing wave decay (via change cross-reef in γ) across a coral reef flat on time-averaged and wave-by-wave bases; and, 2) assess the accuracy of a common wave energy dissipation model on a reef flat using spatially variable γ in the surf zone.

One Tree Reef

One Tree Reef (OTR) is a lagoonal mid-shelf reef in the Capricorn Bunker Group of the Southern Great Barrier Reef (GBR) (Figure 2). OTR receives moderate wave energy with Hopley (1982) reporting a 1.15 m offshore significant wave height (H_{so}) on average for the southern GBR (reanalysis of the offshore wave record is shown in Figure S1). Waves are predominately from the southeast and do not change significantly throughout the year although OTR may be exposed to cyclone events during the summer months (November – March). The reef flats of OTR are emergent during low tide with no interaction between the pelagic and lagoonal environments during this time. Tides are meso-tidal with a maximum tidal range of 3.5 m which result in water depths of 2.1 m over the reef flat (Harris et al., 2014). This study deployed pressure transducers on the southern reef flat (P1-6, Figure 1c), which is dominated by turf and crustose coralline algae, and has minimal live coral cover (Thornborough and Davies, 2011). Coral boulders are randomly dispersed on the reef flat, with a greater accumulation of smaller coral rubble at the lagoonward end of the reef flat (P5-6) (see photos in Supplementary Material Appendix 3). The reef flat is near horizontal or with a mild slope ($tan\beta$) at near the reef crest (P1, $tan\beta = 0.01$), near horizontal at the mid reef flat (P2-3, $tan\beta \approx 0.002$), mildly negatively sloped near the lagoon (P4-5, $tan\beta = -0.01$), and is horizontal on the live coral windrows that have formed on the back-reef sand apron ($tan\beta \approx 0$, Figure 1d).

Methods

Analysis of previous literature

We reviewed all the previously published values of γ – to our knowledge – to examine the variation and average values of γ on coral reef flats. The definition of γ reported, the observation location on the reef flat, and the method used to determine γ were assessed (Table S1 and Supplementary Material). The maximum observed γ and the γ used in calibrated wave models are summarized in Figure 1. These two definitions of γ were selected since maximum observed values of γ in the literature have informed the values used for γ in wave energy dissipation models (e.g. Gourlay, 1994; Gourlay, 1996; Lowe et al., 2005; Massel and Gourlay, 2000; Nelson, 1994) . We categorised values as being derived from one of two main zones on the cross-reef profile: (1) the reef crest or outer surf zone, and (2) the reef flat or inner surf zone (Figure 1 and 2). The average values observed in each zone and in calibrated wave models are shown in Figure 1 and reported in Table S1. Table S1 in the supplementary material shows the full list of publications used in the analysis.

Offshore wave record

The long-term offshore wave climate (H_{so} and T_p) for OTR was defined, for the first time, using the Centre for Australian Weather and Climate Research (CAWCR) Wave Hindcast (1979-2013), which provides hourly wave predictions at 4 arc minute resolution around the Australian coastline (Durrant et al., 2014; Durrant et al., 2013) (Figure S1). The wave hindcast dataset was developed using the WAVEWATCH III spectral wave model (Tolman, 2014) with Climate Forecast System (CFS) atmospheric forcing (Saha et al., 2010). To provide offshore wave conditions at OTR (coordinates 23°30' S, 152°12' E) during the three field sampling periods in 2012, 2014 and 2016, a comparable WAVEWATCH III spectral wave model and CFS forcing was used, the Nearshore Coastal Ocean Wave (NCOW) model (Kinsela et al., 2014), providing wave predictions in the GBR region at 0.25° resolution (Figure 1).

To ensure consistency between the long-term CAWCR Wave Hindcast dataset and the offshore wave model run for the field sampling periods (NCOW), wave height predictions for the 2012 calendar year were compared to recorded waves at a Waverider Buoy station located in 80 m water depth offshore of Byron Bay (500 km SSE from OTR). Both the CAWCR Wave Hindcast and NCOW model performed well against waverider buoy measurements until $H_{so} > 5$ m which is larger than the range of offshore wave heights examined in this study (Figures S3, S4 in Supplementary Material). Extreme storm peak wave heights were under-predicted by both the hindcast dataset and the wave model (Figure S4). This may be attributed to the resolution of the atmospheric forcing data, which limits the capacity to accurately resolve steep coastal wind gradients associated with the land-sea interface (e.g. Kinsela et al., 2014; Sharp et al., 2015). This resolution effect diminishes with increased distance from the coastline, and is not expected to be significant at OTR, which is located 90 km from the Queensland coastline. The comparison shows that at the Byron Bay location, the wave hindcast dataset and wave model provide comparable predictions for significant wave heights up to 5 m (Figure S4). The probability distribution of the offshore wave heights were compared to the Weibull, Gumbel, and Lognormal distributions using the Wave Analysis for Fatigue and Oceanography MATLAB® toolbox (Brodtkorb et al., 2000). The lognormal distribution produced the most accurate description of the offshore wave heights and the mean long-term significant wave height and wave period were computed from this distribution.

Field measurement

Waves were measured during non-storm conditions on the reef flat of OTR on 13-14 December 2012 and 15-16 March 2016 and during a storm event generated by a low to moderate energy cyclone on 30-31 January 2014 (Tropical Cyclone (TC) Dylan, storm conditions). In total almost 120,000 individual waves were measured and analysed. Waves were measured using pressure transducers (PTs, INW Aquistar PT2X) which were deployed on the southern reef flat in a cross-reef transect. PTs logged continuously at a sampling frequency of 8 or 10 Hz, depending on the maximum frequency of the PT. Five PTs were deployed in December 2012 (P1 and 3-6 from reef crest to lagoon) and four in January 2014 and March 2016 (P2-5) (Figure 2c). Repeat deployments were conducted at sites P2, 4, 5, and 6 for the three measurement periods. Data were divided into 15-minute records and records that were not fully submerged for the full 15 minutes were removed.

Data processing and wave statistics

The pressure records from the PTs were low-pass filtered to remove instrument noise, high-pass filtered to separate infragravity effects and then split into 15-minute runs to remove the tidal influence in the record (e.g. Hughes and Moseley, 2007). Pressure attenuation with depth was corrected using methods outlined in Tucker and Pitt (2001). Wave height (H) and wave period (T) were calculated using zero down-crossing analysis, with significant wave height (H_s) calculated for each 15-minute run. Using these data, γ_s, and wave height to water depth for individual waves (γ_w), were calculated using $H_s/\bar{h}$ and H/h_w respectively, where $\bar{h}$ is the mean water depth across the 15-minute run and h_w is the average water depth for an individual wave. γ_s was selected as the time-averaged value of γ due to the widespread use of this term (since H_s is the most common measurement of wave height) when assessing surf zone saturation in field settings (e.g. Power et al., 2010; Raubenheimer et al., 1996).

Wave energy dissipation model

We applied the Alsina and Baldock (2007) and Janssen and Battjes (2007) (hereafter AB07/JB07) random wave breaker dissipation model in combination with frictional dissipation equations (Jonsson, 1966; Swart, 1974) to the southern reef flat of One Tree Reef, using a similar approach to that of Lowe et al. (2005) for coral reefs. The AB07/JB07 follows the approach of Battjes and Janssen (1978) and determines the mean (time-averaged) decay of wave height and energy by applying an energy flux balance across the surf zone. The AB07/JB07 models (that are identical but developed independently) include updated estimates of dissipation in the inner surf zone to remove shoreline singularities of earlier models (Baldock et al., 1998) and correct some of the errors observed by Janssen (2006) and Ruessink et al. (2003) in the inner surf zone. The model can be summarized by:

$$\frac{dEC_g}{dx} = -D_b - D_f \qquad \text{(Eq. 2)}$$

where EC_g is the wave energy flux, D_b is the wave energy dissipation due to breaking (both initial breaking at the breakpoint and ongoing breaking due to bore processes), and D_f is the wave energy dissipation due to bed friction. The wave energy flux is defined as the wave energy multiplied by the wave group velocity:

$$E = \frac{1}{8} pgH_{rms}{}^2 \qquad \text{(Eq. 3)}$$

$$C_g = C\frac{1}{2}\left(1 + \frac{2kh}{sinh2kh}\right) cos\theta \qquad \text{(Eq. 4)}$$

where H_{rms} root-mean-square wave height, C_g is the group velocity normal to the reef crest, C is the wave phase velocity, ρ is the water density, k is the wave number, g is gravitational acceleration, and θ is the incident wave angle. Wave number was determined by solving the dispersion relation for shallow water using the Newton – Raphson iteration method. Since no directional wave information was available in this study, and the model was applied after wave breaking in the inner surf zone, we assume $cos\theta = 1$. This is not strongly limiting since most of the wave refraction will have likely already occurred prior to the wave measurements on the reef flat.

The most common formulation of D_b is to approximate energy dissipation as propagating water bores, first proposed by Lamb (1932), which is then multiplied by the number of broken waves over the total number of waves per unit of the cross-shore distance . The fraction of broken waves is determined by assuming a Rayleigh distribution of waves at each location in the surf zone. This approach includes all processes that lead to energy dissipation such as, boundary shear, friction between the wave roller and wave surface, and turbulence due to breaking. In the AB07/JB07 model, D_b is given by:

$$D_b = \frac{3\sqrt{\pi}}{16}\frac{f\rho g {H_{rms}}^3}{h}\left[1 + \frac{4}{3\sqrt{\pi}}\left({\frac{H_b}{H_{rms}}}^3 + \frac{3}{2}\frac{H_b}{H_{rms}}\right)\exp\left(-{\frac{H_b}{H_{rms}}}^2\right) - \text{erf}\left(\frac{H_b}{H_{rms}}\right)\right] \qquad \text{(Eq. 5)}$$

where f is the dominant frequency of the wave spectrum, H_b breaker wave height ($H_b = \gamma h$), erf is the error function (implemented in MATLAB® here). The loss of wave energy due to bed friction may be large in coral reef environments (Lowe et al., 2005; Monismith et al., 2015) so an additional factor that determines frictional energy loss is required (D_f). The Swart (1974) frictional dissipation equation was used incorporating the wave friction factor (f_w, Jonsson 1966):

$$D_f = \frac{2}{3\pi}\rho f_w U^3 \qquad \text{(Eq. 6)}$$

where U is the near bed orbital velocity determined from linear wave theory.

The two free parameters in the full model are γ (used to define H_b) and f_w. f_w was varied spatially during model calibration between the locations of wave measurement, similar to

Lowe et al. (2005) and Péquignet et al. (2011), resulting in four different zones of roughness on the reef flat. We also calibrated the wave model with a spatially constant f_w value since this method has been used previously on coral reefs (e.g. Harris et al., 2018; Monismith et al., 2013; Pomeroy et al., 2012). Calibration of both parameters was performed by applying the Generalised Likelihood Uncertainty Estimation (GLUE, Beven and Binley (1992)) method for 100,000 model runs, see Simmons et al. (2015) for an example of applying the GLUE method for coastal models. The best fitting value of γ was 0.57 and the values for f_w are shown in Table 1 for the model with spatially varying f_w. For the wave energy dissipation model with a constant f_w, γ = 0.48 and f_w = 0.2.

Results

Reef flat and offshore wave conditions

The long-term offshore wave data indicate that the mean significant offshore wave height ($\overline{H_{so}}$) and offshore wave period ($\overline{T_p}$) for the southern GBR are $\overline{H_{so}}$ = 1.5 m and $\overline{T_p}$ = 6.7 s, which are larger than values reported by Hopley (1982) (Figure S1). The offshore wave height from the NCOW wave model is shown in Figure 3; the average H_s for the 2012, 2014, and 2016 during the measurement periods were 2.6 m, 4.9m, and 1.21 respectively. The conditions during 2012 and 2016 are considered non-storm conditions since $H_s < 3$ m and 2014 considered storm conditions since $H_s > 3$ m (as defined by Lord and Kulmar (2001)).

Waves on the reef flats did not vary with changes in the offshore wave conditions (Figure 3). The time-averaged wave heights on the reef flat during all deployments were depth limited and could mostly be described by local water depth where $H_s = 0.31\bar{h}$ ($\overline{\gamma_s}$ = 0.31, R^2 = 0.96, n = 114726, Figure 4a). However, when examined for each 15-minute run, γ_s varied considerably (Figure 4c). γ_s values had greater variance in shallow water conditions with a maximum value of 0.9 and minimum of 0.05 when $\bar{h} \approx 0.1$ (Figure 4c). These differences were dependent on the measurement location on the reef flat. For measurements closer to the reef crest at the outer reef flat (P1-4) γ_s increased as depth decreased resulting in large γ_s values in shallow water conditions ($\bar{h}$ < 1 m) (Figure 5a). Measurements that were furthest from the reef crest at the inner reef flat (P5-6) showed the opposite trend with γ_s decreasing as depth decreased (Figure 5a). The γ_s values at the outer and inner reef flats for changing depth could be explained by Eq. 7 (R^2 = 0.66, n=495) and Eq. 8 (R^2 = 0.66, n=232) respectively which were derived from exponential regression for $\bar{h} \geq 0.1$ where:

$$\gamma_{s,outer} = 0.61exp(-4.87\bar{h}) + 0.33 \quad \text{(Eq. 7)}$$

$$\gamma_{s,inner} = -0.87exp(-0.07\bar{h}) + 1.06 \quad \text{(Eq. 8)}$$

Eq. 7 and 8 are shown in Figure 5a. The values of γ_s in greater water depths tended towards the mean of γ_s = 0.31 at both the outer and inner reef flat (Figure 4c and 5a). The γ_s values in general decreased as waves propagated across the reef flat and at greater depths (Figure 5a and b). The wave shape and wave deformation also changes during propagation over the reef flat particularly during shallow water conditions (Figure 6 and 7 and Figure S7 in the Supplementary Material).

Wave-by-wave analysis

Large variation in wave height to water depth ratios was also observed on a wave-by-wave basis (Figure 8). The distribution of γ_w showed larger values of up to γ_w = 3, over three times greater than that of the maximum observed values in the time-averaged analysis of γ_s = 0.9 (Figure 8). The trends in γ_s and γ_w values with changing water depths were similar whereby γ_w increased on the outer reef flat (P1-4) and decreased on the inner reef flat (P5-6) as water depth decreased (Figure 8c and d). As such, a greater proportion of individual waves were dissipated at the outer reef flat under shallow water conditions resulting in smaller waves near the lagoon (Figure 8c and d). Maximum γ_w values (γ_{w_max}) also changed with water depth: all recorded waves for the inner reef flat were below a maximum γ_w of 0.5. γ_{w_max} = 0.5 also adequately explained most of the waves for the outer reef flat when h > 1 m (Figure 8d). A value of 0.8 was more appropriate when h < 1 m for the outer reef flats, although γ_{w_max} could also be much higher when h < 0.5 m (Figure 8). The maximum value of γ_w changed throughout the tidal cycle with no one value adequately explaining the limit of wave height to water depth for all water depths and locations (Figure 8).

Discussion

Wave transformation on coral reef flats

Wave conditions on the reef flat were saturated and independent of offshore incident wave height even under cyclone generated swell conditions (Figure 3). Consequently, the significant wave height, averaged for the combined period of all deployments, could be accurately predicted using local water depth ($H_s = 0.31\bar{h}$) (Figure 4a). This is consistent with previous studies that have noted strong correlations between wave heights and water depths on coral reef flats (e.g. Gourlay, 1994; Hardy and Young, 1996; Monismith et al., 2013; Nelson, 1994). Despite the correlation between wave height and water depth observed here (Figure 4a), γ_s was not cross-reef constant and showed considerable variation depending on the location of measurement on the reef flat (Figure 4c and 5a). This clearly shows that there is no single value for γ_s that is applicable for an entire tidal cycle nor for all locations on the coral reef flat. The γ_s values, when averaged for each location from the three measurement periods, were greater on the outer reef flat and decreased as waves propagated across the reef flats towards the lagoon (Figure 5b). The average γ_s values for each location were 0.2 – 0.5 (Figure 5b) and are similar to previous observations of reef flat waves (Hardy et al., 1990, Table S1) particularly at the inner reef flat where the maximum wave-by-wave γ (γ_{w_max}) is 0.5 (Figure 8b and d), i.e., the same value observed by Nelson (1994), Gourlay (1994) and many subsequent studies (Figure 1 and Table S1).

However, the average γ_s values from the entire measurement period mask significant detail in the variation of γ_s with changing depth that has not been observed in previous studies (Figure 4c and 5a). At the inner reef flat, on near horizontal or mild negative slopes, $\gamma_s = 0.5$ and therefore $H_s = 0.5h$ effectively defined the upper limit of wave heights and therefore showed that waves were saturated. The outer reef flat maximum wave heights could also be predicted by $H_s = 0.5h$ when $h > 1 – 1.5$ m. However, during shallow water at the outer reef flat when h approached zero, H_s did not decrease at the same rate, leading to high values of γ_s. A similar increase in γ_s was observed by Raubenheimer et al. (1996) and Baldock et al. (1998) in the shallow nearshore zones of steep beaches due to increased breaker dissipation as "shore breaks". This may also explain the increase in γ_s during shallower water near the reef crest and the break-down of wave height predictions based on assumptions of depth-limited waves heights (e.g. Equation 1). The disparity between the high γ_s values on the outer reef flat ($\gamma_s > 0.8$) and the low γ_s values on the inner reef flat ($\gamma_s < 0.1$) in shallow water indicated that most of the wave energy was dissipated on the outer reef flat and reef crest (Figure 8d). This may be due to both increased breaker dissipation but also greater frictional dissipation at the outer reef flat leading smaller than expected waves in the inner reef flat when assuming depth limited wave heights. The much higher calibrated values of f_w in the wave energy dissipation model at the outer reef flat when compared to the inner reef flat may support this conclusions (Table 1). The high f_w values would also suggest that the outer reef flat has higher structural complexity and, while higher coral cover was observed on the reef flats in this location, in absence of any direct quantitative measurement it is not possible to define the benthic ecological assemblages that led to the high f_w values. The low γ_s values at the inner reef flat during shallow water is most likely also due to the slight increase in local water depth due to the mild negative slope in this region that does not correspond with an increase in H. Despite the inaccuracy of depth limited assumptions during shallow water at both the inner and outer reef flat, the surf zone was still characterized by saturated conditions as local wave heights were not influenced by changes in offshore wave conditions.

In order to assess the effects of the observed changes in γ_s on wave energy dissipation models, we applied the modified AB07/JB07 wave energy dissipation model described above to the data recorded in 2012 (Figure 9a and b). The deployment record from 2012 was selected since it covers most of the full width of the reef flat from P1-P6 (without P2 due to equipment failure). We find that the model shows good overall agreement with regards to the average rate of wave energy dissipation across the reef flat (Figure 9) suggesting that small γ_s values at the inner reef flat are indeed due to the enhanced breaker dissipation in shallow water at the outer reef flat. However, there were significant differences between the measured and modelled wave heights for outer and inner reef flat (Figure 9c). The model tended to under predict wave height in shallow water and over predict wave height in deeper water at the outer reef flat (Figure 9c). For the inner reef flat, wave heights were generally over-predicted. Despite these inaccuracies in the model, most discrepancies for the inner reef flat region could be corrected by spatially varying the values of reef roughness (f_w) across the reef flat; an approach that is not available for models that use a spatially constant f_w (Table 1, Figure 9 and Supplementary Material). In contrast, allowing for spatially varying roughness coefficients only marginally improved the accuracy of breaker dissipation at the outer reef flat, particularly during shallow water (Figure 9b and Supplementary Material). This indicates that, while random wave energy dissipation models can be successfully tuned to calculate wave energy dissipation on the reef flat, they may inaccurately represent breaker dissipation near the reef crest.

The errors observed in the models are most likely linked to the observed cross-reef and depth variable values of γ observed in this study (Figure 5) and may highlight the difficulties in applying wave energy dissipation models to coral reef environments with steep or complex bathymetries (Salmon and Holthuijsen, 2015). We also note that the choice of spatially varying or constant f_w within the wave model resulted in different values of γ and f_w being assigned during model calibration. This is not unexpected but it indicates that γ and f_w produced from model calibrations are dependent on the mechanics of the wave energy dissipation model selected and potentially on each other. Due to the many varied approaches taken to determine γ and f_w in the literature, including a wide range of f_w values applied to the same coral reef (e.g. f_w = 0.3-7, Gove et al. (2015), Monismith et al. (2015), Rogers et al. (2016)) it is clear that there is not yet a consistent method for determining the free parameters in wave energy dissipation models of γ and f_w (or equivalent roughness coefficient), nor are there universal values that can be assigned to coral reefs (Rosman and Hench, 2011).

In order to further explain the variability in γ_s, a number of additional wave parameters were examined similar to the approach taken by Ruessink et al. (2003) (Supplementary Material). We found a correlation was between wave deformation and γ_s (for $\gamma_s < 0.6$) with the least square linear regression fit given by:

$$\gamma_s = -0.2def + 0.53 \qquad \text{for } \gamma_s < 0.6 \qquad \text{(Eq. 9)}$$

where *def* is the time-averaged wave deformation, which is the ratio of the time between the zero up-crossing and wave crest (*a*) and the time between the wave crest and zero down-crossing (*b*) obtained from the pressure time series (*def* = *a*/*b*) (Cowell, 1982) (Figure 6 and

Figure S6 in Supplementary Material). This result suggests that the larger γ_s values are due to waves with higher deformation values that Cowell (1982) defined as ‘hyper crested’ waves and that more closely resembled surf zone bores (Figure 7). Conversely, as waves propagate into the inner reef flat they reduce in deformation potentially indicating the reforming of wave shape or that the rate of energy dissipation due to breaking decreases through a reduction in bore strength (Figure 6 and 7). However, Eq. 9 was still unable to describe the maximum values of γ_s (e.g. $\gamma_s > 0.6$) in the outer reef flat during shallow water. As such, there are most likely additional mechanisms driving the largest values of γ_s such as the rate of energy dissipation in the surf zone when compared to rate of change in water depth and offshore wave steepness that is beyond the current data set of this study (Battjes and Stive, 1985; Raubenheimer et al., 1996).

The form of γ_s presented in Eq. 13 can only be calculated through wave-by-wave measurements, which are shown here to provide insights into the controls of wave decay for individual waves during propagation across reef flats. Depth was the primary control in defining the maximum height of individual waves, despite the considerable variation in wave height. This has not always been observed in previous studies, for example unsaturated surf has been observed for individual waves on siliciclastic beaches (Power et al., 2010). However, in a similar trend to those observed in the time-averaged results, the wave-by-wave maximum wave height to water depth ratio (γ_{w_max}) was not cross-reef constant under shallow water conditions. Greater wave decay across the surf zone was observed during shallow water with much larger waves observed in the outer reef flat when compared to the inner reef flat. A limiting γ_w value of $\gamma_{w\_max} = 0.5$ explained most of the wave record for the inner reef flat, particularly at higher tidal stages (Figure 8). When $h > 1$ – 1.5 m, $\gamma_{w\_max} = 0.5$ adequately described wave conditions on the outer reef flat (Figure 8). However, under shallow water a limiting γ_{w_max} value of 1.5 explained most of the waves with some instances of $\gamma_{w\_max} \approx 3$ also observed under shallow water (Figure 8 and Figure S7 in Supplementary Material). This indicates that there can be individual waves three times larger than what is suggested by time-averaged results. Waves such as this are likely to be important non-linear mechanisms of change in coral reefs, and have the potential to dislodge of coral colonies from reef substrate, however, the effects of these individual waves have not been examined in detail to date.

Conclusions

The results here show that surf zones are saturated on the southern reef flat of One Tree Reef but not necessarily depth limited. This result is consistent with most reef flats based on our literature review. Wave height to water depth ratios were shown to vary most during shallow water; increasing on the outer reef flat ($\gamma_s > 0.85$) and decreasing on the inner reef flat ($\gamma_s < 0.1$). In contrast, wave height to water depth ratios were consistent across the entire reef flat ($\gamma_s = 0.31$, $\gamma_{w\_max} = 0.5$) under greater water depths and were close to previously reported values. The difference in γ_s between the inner and outer reef flats was also observed in the wave-by-wave analysis and is indicative of increased wave energy dissipation under shallow water due to wave breaking and bed friction. The effects of cross-reef and depth variable γ on a random wave energy dissipation model was also examined. The model results were accurate, but showed errors that were most likely due to the cross-reef variability of γ observed in the wave data. This led to inaccurate descriptions of wave conditions, primarily for the outer reef flat. Our results highlight the challenges when using wave energy dissipation models in environments with steep and complex bathymetry such as coral reefs we show the importance of accurate model calibration with site-specific field data in such systems.

Acknowledgements

DH is funded by Institutional Strategy of the University of Bremen, funded by the German Excellence Initiative (ABPZuK-03/2014) as part of MARUM and by ZMT, the Center for Tropical Marine Ecology, University of Bremen. DH was also funded by a Leibniz ZMT core budget funding (70005) and a new staff grant at The University of Queensland. AVC is funded by ARC Future Fellowship (FT100100215). One Tree Island is a field station run by the University of Sydney. Online documentation for pressure record filtering and wave model development by Urs Neumeier and Falk Feddersen is also acknowledged. We would like to thank the three reviewers who helped improve this manuscript during the review process.

References

Alsina, J.M., Baldock, T.E., 2007. Improved representation of breaking wave energy dissipation in parametric wave transformation models. Coastal Engineering 54, 765-769.

Baldock, T.E., Holmes, P., Bunker, S., Van Weert, P., 1998. Cross-shore hydrodynamics within an unsaturated surf zone. Coastal Engineering 34, 173-196.

Battjes, J., Janssen, J., 1978. Energy loss and set-up due to breaking of random waves. Proceedings of 14th International Conference on Coastal Engineering 1.

Battjes, J., Stive, M., 1985. Calibration and verification of a dissipation model for random breaking waves, Coastal Engineering 1984, pp. 649-660.

Beaman, R., 2010. Project 3DGBR: A high-resolution depth model for the Great Barrier Reef and Coral Sea. Marine and Tropical Sciences Research Facility (MTSRF) Project 2.5i.1a Final Report, MTSRF, Cairns, Australia, p. pp. 13.

Beven, K., Binley, A., 1992. The future of distributed models: model calibration and uncertainty prediction. Hydrological Processes 6, 279-298.

Brodtkorb, P.A., Johannesson, P., Lindgren, G., Rychlik, I., Ryden, J., Sjö, E., 2000. WAFO-a Matlab toolbox for analysis of random waves and loads, The Tenth International Offshore and Polar Engineering Conference. International Society of Offshore and Polar Engineers.

Cowell, P.J., 1982. Breaker stages and surf structure on beaches. University of Sydney.

Demirbilek, Z., Nwogu, O.G., 2007. Boussinesq modeling of wave propagation and runup over fringing coral reefs, model evaluation report. DTIC Document.

Durrant, T.H., Greenslade, D., Hemer, M., Trenham, C., 2014. A Global Wave Hindcast Focussed on the Central and South Pacific. CAWCR Technical Report No. 070, p. 34 pp.

Durrant, T.H., Hemer, M., Trenham, C., Greenslade, D., 2013. CAWCR Wave Hindcast 1979-2010. v7. CSIRO. Data Collection. 10.4225/08/523168703DCC5.

Gourlay, M.R., 1994. Wave transformation on a coral reef. Coastal Engineering 23, 17-42.

Gourlay, M.R., 1996. Wave set-up on coral reefs. 2. set-up on reefs with various profiles. Coastal Engineering 28, 17-55.

Gove, J.M., Williams, G.J., McManus, M.A., Clark, S.J., Ehses, J.S., Wedding, L.M., 2015. Coral reef benthic regimes exhibit non-linear threshold responses to natural physical drivers. Marine Ecology Progress Series 522, 33-48.

Hardy, T., Young, I., Nelson, R., Gourlay, M., 1990. Wave attenuation on an offshore coral reef. Coastal Engineering Proceedings 1.

Hardy, T.A., Young, I.R., 1996. Field study of wave attenuation on an offshore coral reef. J. Geophys. Res. 101, 14311-14326.

Harris, D.L., Rovere, A., Casella, E., Power, H., Canavesio, R., Collin, A., Pomeroy, A., Webster, J.M., Parravicini, V., 2018. Coral reef structural complexity provides important coastal protection from waves under rising sea levels. Science Advances 4.

Harris, D.L., Vila-Concejo, A., Webster, J.M., 2014. Geomorphology and sediment transport on a submerged back-reef sand apron: One Tree Reef, Great Barrier Reef. Geomorphology 222, 132-142.

Harris, D.L., Vila-Concejo, A., Webster, J.M., Power, H.E., 2015. Spatial variations in wave transformation and sediment entrainment on a coral reef sand apron. Marine Geology 363, 220-229.

Hearn, C.J., 1999. Wave-breaking hydrodynamics within coral reef systems and the effect of changing relative sea level. Journal of Geophysical Research: Oceans 104, 30007-30019.

Hoegh-Guldberg, O., Mumby, P.J., Hooten, A.J., Steneck, R.S., Greenfield, P., Gomez, E., Harvell, C.D., Sale, P.F., Edwards, A.J., Caldeira, K., Knowlton, N., Eakin, C.M., Iglesias-Prieto, R., Muthiga, N., Bradbury, R.H., Dubi, A., Hatziolos, M.E., 2007. Coral Reefs Under Rapid Climate Change and Ocean Acidification. Science 318, 1737-1742.

Hopley, D., 1982. Geomorphology of the Great Barrier Reef: Quaternary development of coral reefs. John Wiley and Sons, New York.

Hughes, M.G., Moseley, A.S., 2007. Hydrokinematic regions within the swash zone. Continental Shelf Research 27, 2000-2013.

Janssen, T.T., 2006. Nonlinear surface waves over topography. TU Delft, Delft University of Technology.

Janssen, T.T., Battjes, J.A., 2007. A note on wave energy dissipation over steep beaches. Coastal Engineering 54, 711-716.

Jonsson, I.G., 1966. Wave boundary layers and friction factors, Proceedings of the 10th International Coastal Engineering Conference, Tokyo, Japan, pp. 109-148.

Kinsela, M., Taylor, D., Treloar, D., Dent, J., Garber, S., Mortlock, T., Goodwin, I., 2014. NSW coastal ocean wave model: Investigating spatial and temporal variability in coastal wave climates, 23rd New South Wales Coastal Conference, Ulladulla.

Lamb, H., 1932. Hydrodynamics. Cambridge University Press, Cambridge.

Longuet-Higgins, M.S., 1974. On the Mass, Momentum, Energy and Circulation of a Solitary Wave. Proceedings of the Royal Society of London A: Mathematical, Physical and Engineering Sciences 337, 1-13.

Lord, D., Kulmar, M., 2001. The 1974 Storms Revisited: 25 Years Experience in Ocean Wave Measurement Along the South East Australian Coast, Coastal Engineering Conference. ASCE American Society of Civil Engineers, pp. 559-572.

Lowe, R.J., Falter, J.L., Bandet, M.D., Pawlak, G., Atkinson, M.J., Monismith, S.G., Koseff, J.R., 2005. Spectral wave dissipation over a barrier reef. Journal of Geophysical Research: Oceans 110, C04001.

Massel, S.R., Gourlay, M.R., 2000. On the modelling of wave breaking and set-up on coral reefs. Coastal Engineering 39, 1-27.

McCowan, J., 1891. VII. On the solitary wave. Philosophical Magazine Series 5 32, 45-58.

Monismith, S.G., 2007. Hydrodynamics of Coral Reefs. Annual Review of Fluid Mechanics 39, 37-55.

Monismith, S.G., Herdman, L.M.M., Ahmerkamp, S., Hench, J.L., 2013. Wave Transformation and Wave-Driven Flow across a Steep Coral Reef. Journal of Physical Oceanography 43, 1356-1379.

Monismith, S.G., Rogers, J.S., Koweek, D., Dunbar, R.B., 2015. Frictional wave dissipation on a remarkably rough reef. Geophysical Research Letters 42, 2015GL063804.

Nelson, R.C., 1987. Design wave heights on very mild slopes - an experimental study. Australian Journal of Civil Engineering 29.

Nelson, R.C., 1994. Depth limited design wave heights in very flat regions. Coastal Engineering 23, 43-59.

Péquignet, A.-C., Becker, J.M., Merrifield, M.A., Boc, S.J., 2011. The dissipation of wind wave energy across a fringing reef at Ipan, Guam. Coral Reefs 30, 71-82.

Pomeroy, A., Lowe, R., Symonds, G., Van Dongeren, A., Moore, C., 2012. The dynamics of infragravity wave transformation over a fringing reef. Journal of Geophysical Research: Oceans 117, C11022.

Power, H.E., Hughes, M.G., Aagaard, T., Baldock, T.E., 2010. Nearshore wave height variation in unsaturated surf. Journal of Geophysical Research: Oceans 115, C08030.

Power, H.E., Hughes, M.G., Baldock, T.E., 2015. A novel method for tracking individual waves in the surf zone. Coastal Engineering 98, 26-30.

Raubenheimer, B., Guza, R.T., Elgar, S., 1996. Wave transformation across the inner surf zone. Journal of Geophysical Research: Oceans 101, 25589-25597.

Rogers, J.S., Monismith, S.G., Koweek, D.A., Dunbar, R.B., 2016. Wave dynamics of a Pacific Atoll with high frictional effects. Journal of Geophysical Research: Oceans 121, 350-367.

Rosman, J.H., Hench, J.L., 2011. A framework for understanding drag parameterizations for coral reefs. J. Geophys. Res.: Oceans 116, n/a-n/a.

Ruessink, B.G., Walstra, D.J.R., Southgate, H.N., 2003. Calibration and verification of a parametric wave model on barred beaches. Coastal Engineering 48, 139-149.

Saha, S., Moorthi, S., Pan, H.-L., Wu, X., Wang, J., Nadiga, S., Tripp, P., Kistler, R., Woollen, J., Behringer, D., Liu, H., Stokes, D., Grumbine, R., Gayno, G., Wang, J., Hou, Y.-T., Chuang, H.-Y., Juang, H.-M.H., Sela, J., Iredell, M., Treadon, R., Kleist, D., Van

Delst, P., Keyser, D., Derber, J., Ek, M., Meng, J., Wei, H., Yang, R., Lord, S., Van Den Dool, H., Kumar, A., Wang, W., Long, C., Chelliah, M., Xue, Y., Huang, B., Schemm, J.-K., Ebisuzaki, W., Lin, R., Xie, P., Chen, M., Zhou, S., Higgins, W., Zou, C.-Z., Liu, Q., Chen, Y., Han, Y., Cucurull, L., Reynolds, R.W., Rutledge, G., Goldberg, M., 2010. The NCEP Climate Forecast System Reanalysis. Bulletin of the American Meteorological Society 91, 1015-1057.

Sallenger, A.H., Holman, R.A., 1985. Wave energy saturation on a natural beach of variable slope. Journal of Geophysical Research: Oceans 90, 11939-11944.

Salmon, J., Holthuijsen, L., 2015. Modeling depth-induced wave breaking over complex coastal bathymetries. Coastal Engineering 105, 21-35.

Saunders, M.I., Leon, J.X., Callaghan, D.P., Roelfsema, C.M., Hamylton, S., Brown, C.J., Baldock, T., Golshani, A., Phinn, S.R., Lovelock, C.E., Hoegh-Guldberg, O., Woodroffe, C.D., Mumby, P.J., 2014. Interdependency of tropical marine ecosystems in response to climate change. Nature Clim. Change 4, 724-729.

Sharp, E., Dodds, P., Barrett, M., Spataru, C., 2015. Evaluating the accuracy of CFSR reanalysis hourly wind speed forecasts for the UK, using in situ measurements and geographical information. Renewable Energy 77, 527-538.

Simmons, J.A., Marshall, L.A., Turner, I.L., Splinter, K.D., Cox, R.J., Harley, M.D., Hanslow, D.J., Kinsela, M.A., 2015. A more rigorous approach to calibrating and assessing the uncertainty of coastal numerical models, Australasian Coasts & Ports Conference 2015:

22nd Australasian Coastal and Ocean Engineering Conference and the 15th Australasian Port and Harbour Conference. Engineers Australia and IPENZ, p. 821.

Storlazzi, C.D., Brown, E.K., Field, M.E., Rodgers, K., Jokiel, P.L., 2005. A model for wave control on coral breakage and species distribution in the Hawaiian Islands. Coral Reefs 24, 43-55.

Storlazzi, C.D., Elias, E.P.L., Berkowitz, P., 2015. Many Atolls May be Uninhabitable Within Decades Due to Climate Change. Scientific Reports 5, 14546.

Swart, D.H., 1974. Offshore sediment transport and equilibrium beach profiles. Delft Hydraulics Laboratory Publication No. 131.

Thornborough, K.J., Davies, P.J., 2011. Reef Flats, in: Hopley, D. (Ed.), Encyclopedia of Modern Coral Reefs: Structure, Form and Process. Springer, Dordrecht, New York.

Thornton, E.B., Guza, R.T., 1982. Energy saturation and phase speeds measured on a natural beach. Journal of Geophysical Research: Oceans 87, 9499-9508.

Thornton, E.B., Guza, R.T., 1983. Transformation of wave height distribution. Journal of Geophysical Research: Oceans 88, 5925-5938.

Tolman, H.L., 2014. User manual and system documentation of WAVEWATCH III R version 4.07. NOAA/NWS/NCEP/MMAB Tech. Note 222.

Tucker, M.J., Pitt, E.G., 2001. Waves in ocean engineering. Elsevier, Amsterdam.

Williams, G.J., Smith, J.E., Conklin, E.J., Gove, J.M., Sala, E., Sandin, S.A., 2013. Benthic communities at two remote Pacific coral reefs: effects of reef habitat, depth, and wave energy gradients on spatial patterns. PeerJ 1, e81.

Figure Captions

Figure 1. Average wave height to water depth ratios (γ) reported in previous literature based on location of measurement on coral reefs and those derived from wave model calibration. The reported values for both the maximum observed γ and the γ used in calibrated wave models are shown here. The number of observations is shown inside the bars. Errors bars represent one standard deviation. Full data are shown in full in Table S1 and S2 in the supplementary material.

Figure 2. Location of field site and deployment of pressure transducers (PTs). (A) Location of One Tree Reef (in green) off the southeast coast of Queensland (QLD), Australia; (B) WorldView-2 satellite image combined digital elevation model from Harris et al. (2014) and Beaman (2010) with the location of pressure transducer (PT) deployments shown in the red box; (C) cross-reef schematic of PT deployment locations with mean sea level (MSL) shown in blue; and, (D) aerial view of PT locations on the reef flat with red line showing location of transect in (C).

Figure 3. (A) Offshore wave height (H_o, from NCOW (Kinsela et al. 2014)) during each of the measurement periods compared to the recorded reef flat significant wave height (H_s) ; (B) significant wave height to water depth ratios (γ_s) for all measurement locations during each of the measurement periods compared to H_o. Note the non-continuous nature of the x-axis.

Figure 4. Wave characteristics compared to water depth at each location for the three measurement periods where faded colours are averages for the 15-minute data records for all measurement locations and dark colours are averages for depth bins of 0.2 m: (A) significant wave height with the mean ratio of significant wave height (H_s) to water depth

($\bar{h}$, $\gamma_s = H_s/\bar{h}$ = 0.31) shown by the black line; (B) zero down-crossing wave period (*T*); and, (C) γ_s. The dashed line in (C) corresponds to the slope of the line of best fit in (A).

Figure 5. (A) Ratio of significant wave height to water depth (γ_s) compared to water depth at each location. Faded colours are averages for 15-minute data records and dark colours are averages for depth bins of 0.2 m. Error bars show standard deviation for the binned data. The equations for the magenta and green lines are Eq. 7 and 8 respectively. (B) Average γ_s from all measurements for P1-P6 and the reef flat topography. Shaded area shows the standard deviation.

Figure 6. The relationship between γ_s and wave deformation (*def*) for the outer (P1-4, in magenta) and inner reef flat (P5-6, in green). The linear regression for $\gamma_s < 0.6$ is shown by the black line (Eq. 9). The circle markers are the values excluded from the linear regression.

Figure 7. Example time series of the water surface (η) from the pressure record during the 2014 deployment from P2-5. Note the different scales on the y-axis.

Figure 8. Wave by wave analysis for the 2012 (blue), 2014 (red), and 2016 (black) measurement periods (A and B). Wave by wave analysis for the six measurement locations (P1-6) on the reef flat recorded during all three measurement periods (C and D). (A) Individual wave heights (*H*) compared to the still water level for individual waves (h_w) (see panel (B) for legend for dashed lines); (B) The ratio of *H* to h_w (γ_w) compared to h_w. Faded colours are averages for 15-minute data records and dark colours are averages for depth bins of 0.2 m. Error bars show standard deviation for the binned data (see panel (A) for legend for points); (C) Individual wave heights (*H*) compared to the mean water depth of the wave (h_w) (see panel (D) for legend for points and panel (B) for legend for dashed lines); and (D) the ratio of *H* to h_w (γ_w) compared to h_w (see panel (B) for legend for dashed lines).

Figure 9. (A) Average cross-reef modelled and measured root-mean-square wave height (H_{rms}); (B) Comparison of measured and modelled waves for the entire deployment record of 2012 with a spatially varying wave friction factor (f_w) shown in Table 1 (see panel (C) for legend); and, (C) a constant f_w value. The inner reef flat is in green and outer reef flat in magenta. The values used for γ and f_w are shown in panels (B) and (C).

Table Captions

Table 1. The calibrated wave friction factor (f_w) used in the wave energy dissipation model (Equation 2) for the regions between the five measurement location in 2012 (Equation 2)

Figures

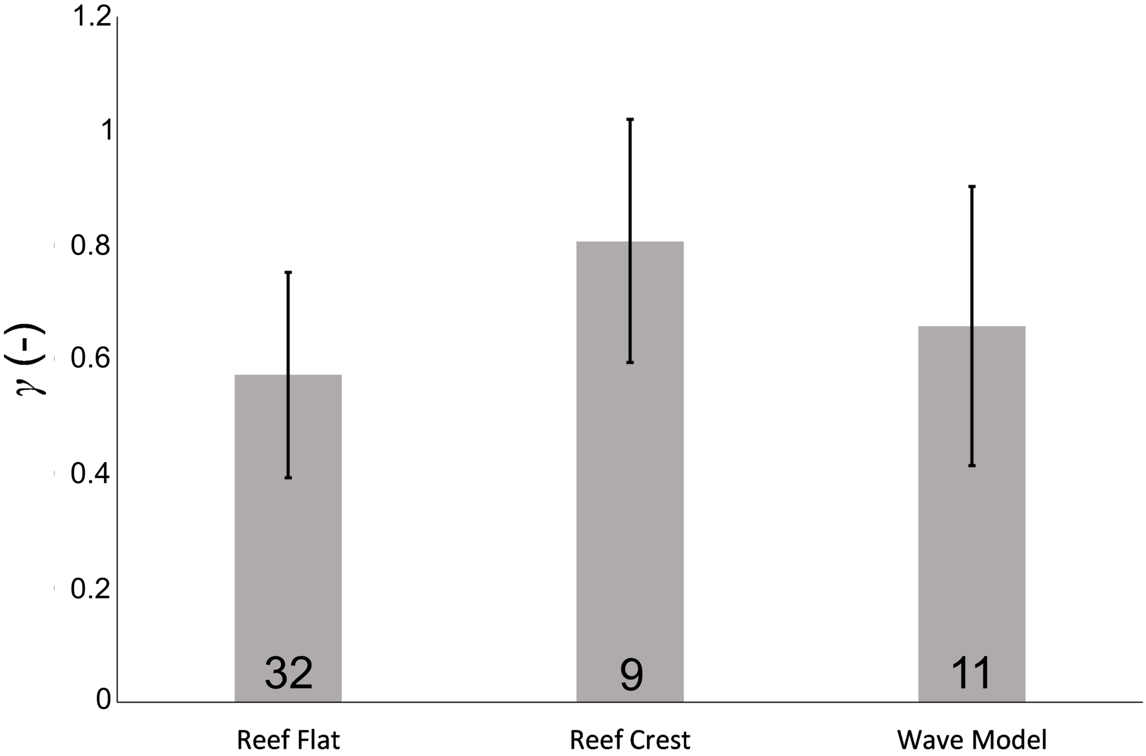

Figure 1. Average wave height to water depth ratios (γ) reported in previous literature based on location of measurement on coral reefs and those derived from wave model calibration. The reported values for both the maximum observed γ and the γ used in calibrated wave models are shown here. The number of observations is shown inside the bars. Errors bars represent one standard deviation. Full data are shown in full in Table S1 and S2 in the supplementary material.

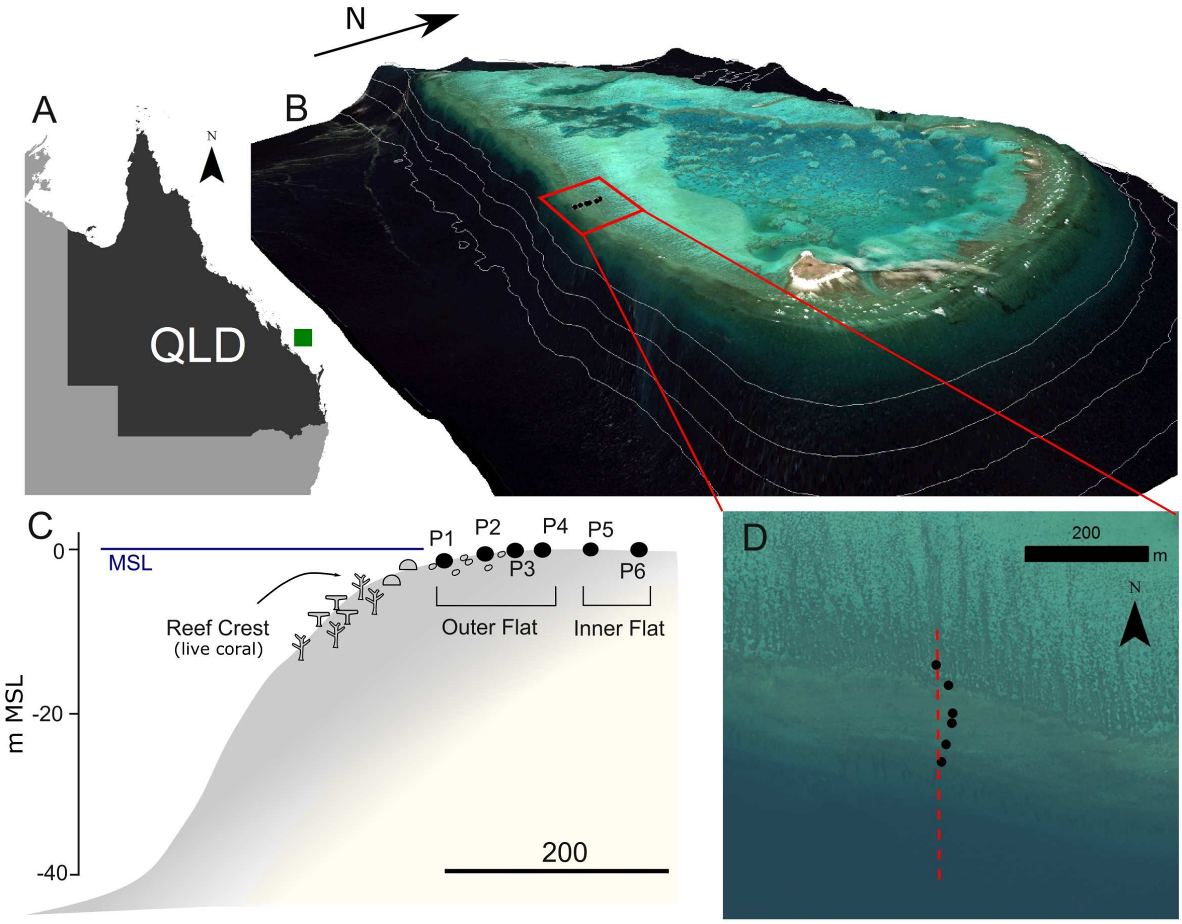

Figure 2. Location of field site and deployment of pressure transducers (PTs). (A) Location of One Tree Reef (in green) off the southeast coast of Queensland (QLD), Australia; (B) WorldView-2 satellite image combined digital elevation model from Harris et al. (2014) and Beaman (2010) with the location of pressure transducer (PT) deployments shown in the red box; (C) cross-reef schematic of PT deployment locations with mean sea level (MSL) shown in blue; and, (D) aerial view of PT locations on the reef flat with red line showing location of transect in (C).

Table 1. The calibrated wave friction factor (f_w) used in the wave energy dissipation model for the regions between the five measurement location in 2012.

	f_w
P1-3	0.29
P3-4	0.18
P4-5	0.05
P5-6	0.11

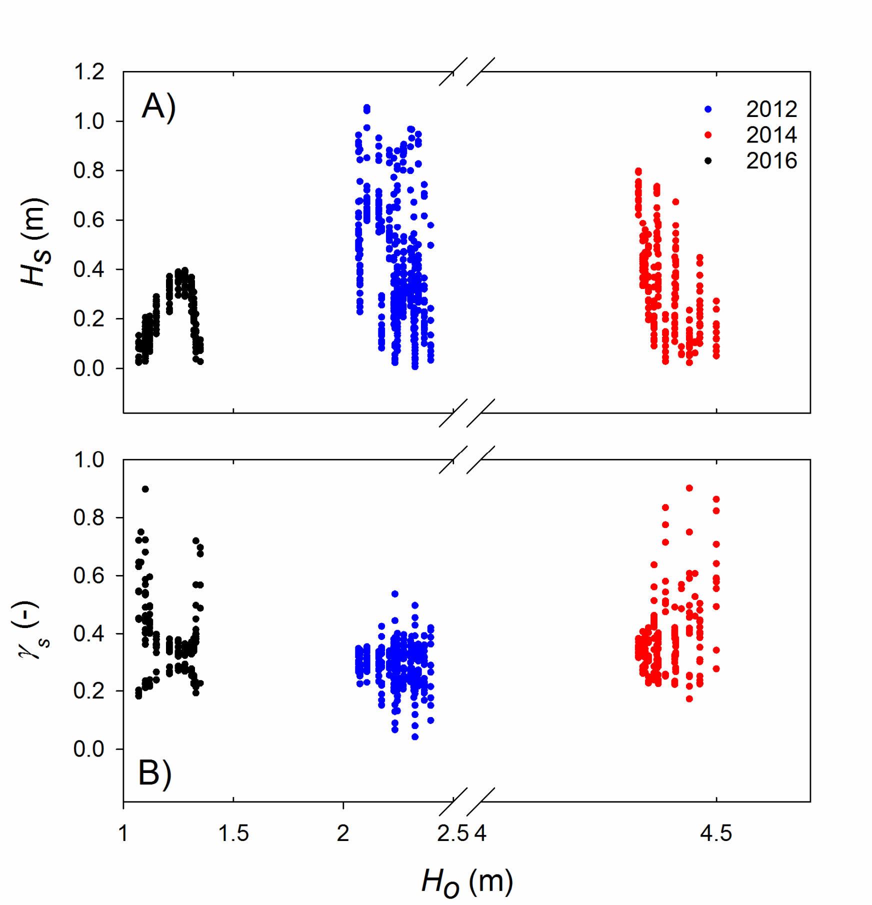

Figure 3. (A) Offshore wave height (H_o, from NCOW (Kinsela et al. 2014)) during each of the measurement periods compared to the recorded reef flat significant wave height (H_s) ; (B) significant wave height to water depth ratios (γ_s) for all measurement locations during each of the measurement periods compared to H_o. Note the non-continuous nature of the x-axis.

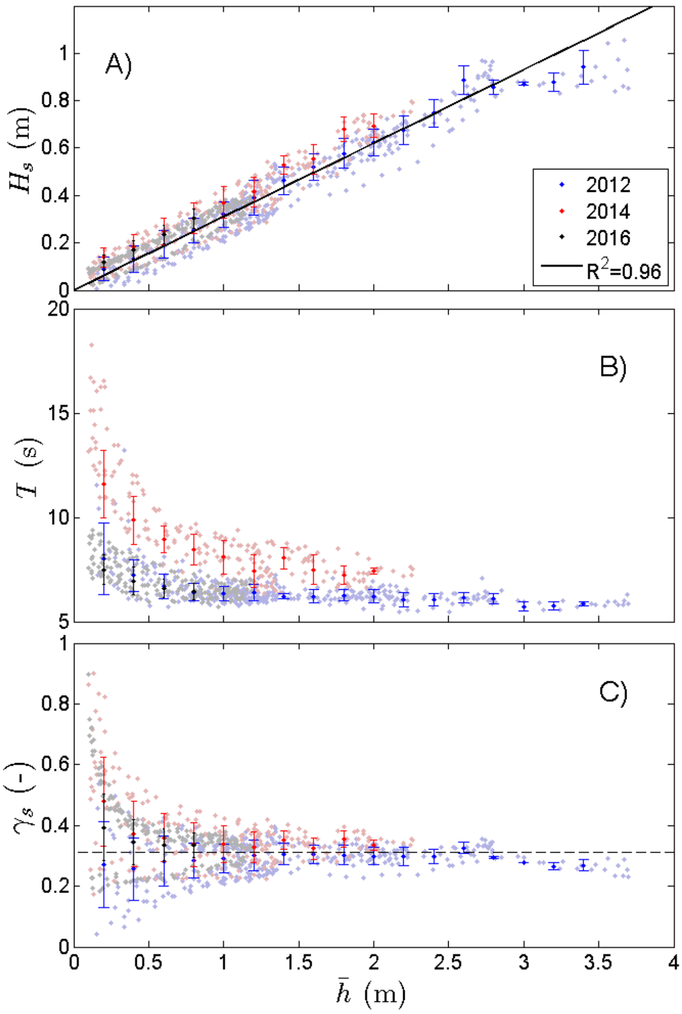

Figure 4. Wave characteristics compared to water depth at each location for the three measurement periods where faded colours are averages for the 15-minute data records for all measurement locations and dark colours are averages for depth bins of 0.2 m: (A) significant wave height with the mean ratio of significant wave height (H_s) to water depth ($\bar{h}$, γ_s= $H_s/\bar{h}$ = 0.31) shown by the black line; (B) zero down-crossing wave period (T); and, (C) γ_s. The dashed line in (C) corresponds to the slope of the line of best fit in (A).

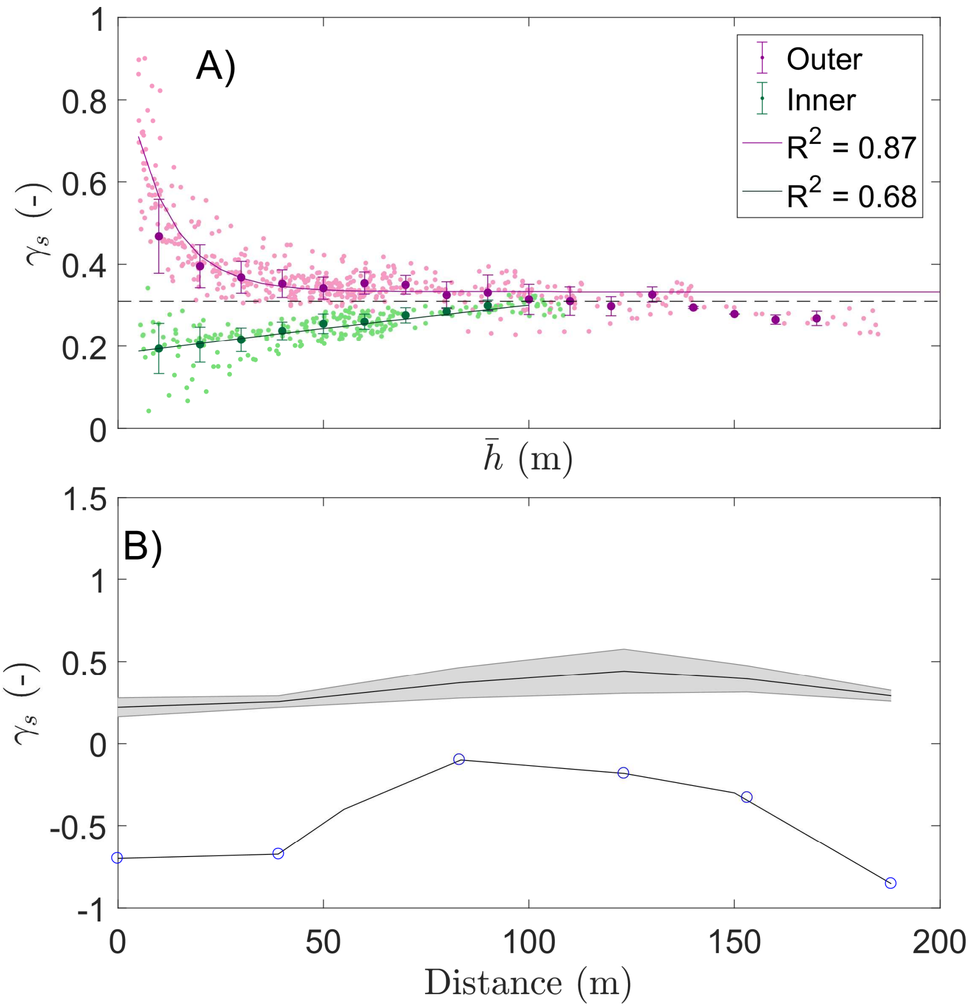

701

702 **Figure 5**. (A) Ratio of significant wave height to water depth (γ_s) compared to water depth
703 at each location. Faded colours are averages for 15-minute data records and dark colours are
704 averages for depth bins of 0.2 m. Error bars show standard deviation for the binned data.
705 The equations for the magenta and green lines are Eq. 7 and 8 respectively. (B) Average γ_s
706 from all measurements for P1-P6 and the reef flat topography. Shaded area shows the
707 standard deviation.

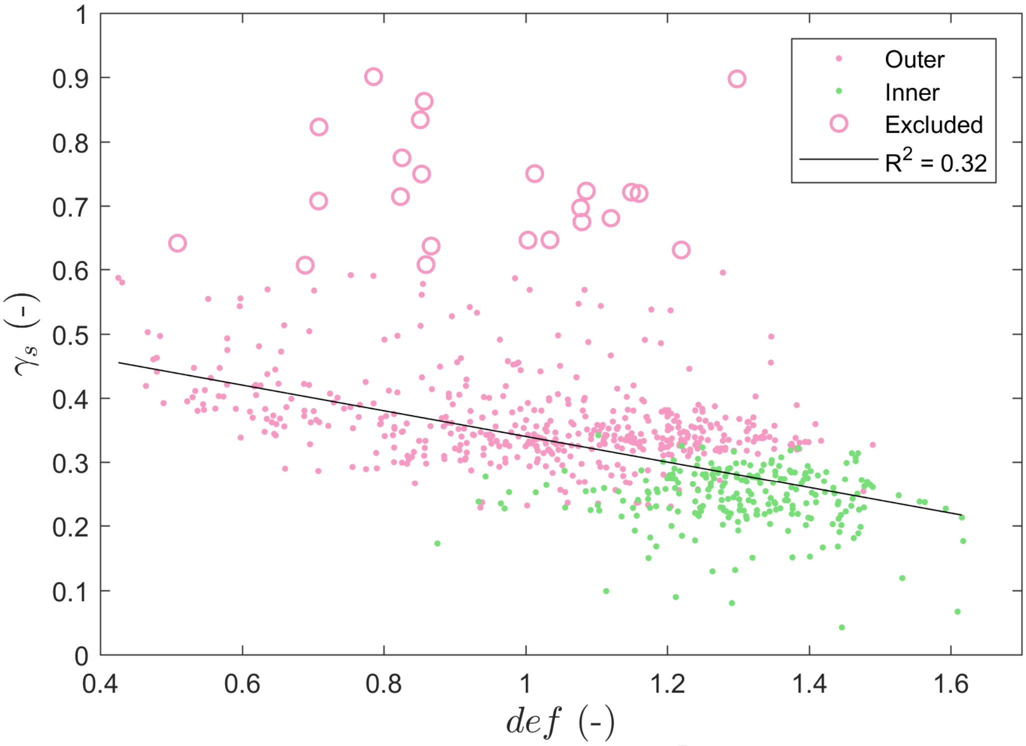

Figure 6. The relationship between γ_s and wave deformation (*def*) for the outer (P1-4, in magenta) and inner reef flat (P5-6, in green). The linear regression for $\gamma_s < 0.6$ is shown by the black line (Eq. 9). The circle markers are the values excluded from the linear regression.

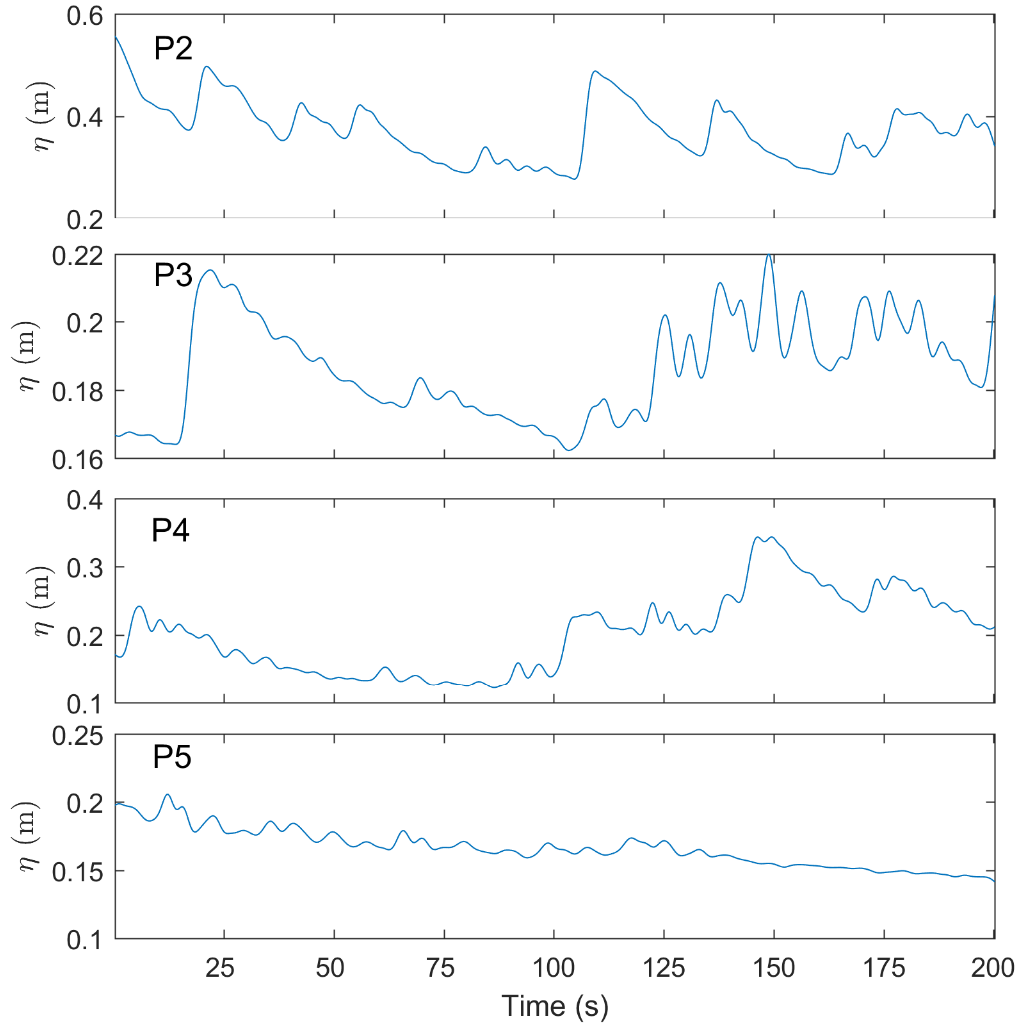

Figure 7. Example time series of the water surface (η) from the pressure record during the 2014 deployment from P2-5. Note the different scales on the y-axis.

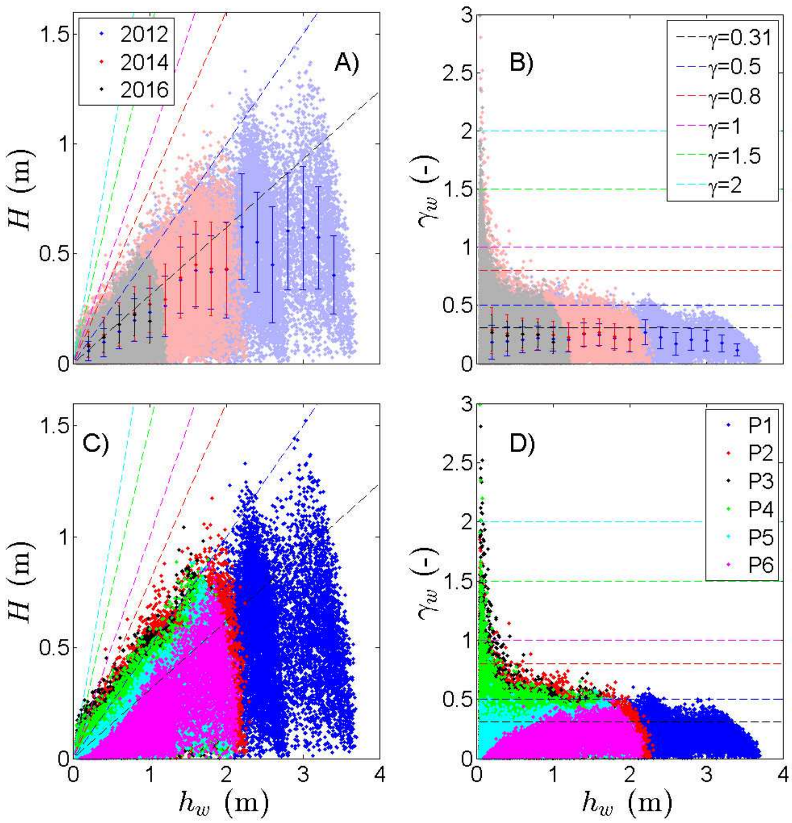

Figure 8. Wave by wave analysis for the 2012 (blue), 2014 (red), and 2016 (black) measurement periods (A and B). Wave by wave analysis for the six measurement locations (P1-6) on the reef flat recorded during all three measurement periods (C and D). (A) Individual wave heights (H) compared to the still water level for individual waves (h_w) (see panel (B) for legend for dashed lines); (B) The ratio of H to h_w (γ_w) compared to h_w. Faded colours are averages for 15-minute data records and dark colours are averages for depth bins of 0.2 m. Error bars show standard deviation for the binned data (see panel (A) for legend for points); (C) Individual wave heights (H) compared to the mean water depth of the wave (h_w) (see panel (D) for legend for points and panel (B) for legend for dashed lines); and (D) the ratio of H to h_w (γ_w) compared to h_w (see panel (B) for legend for dashed lines).

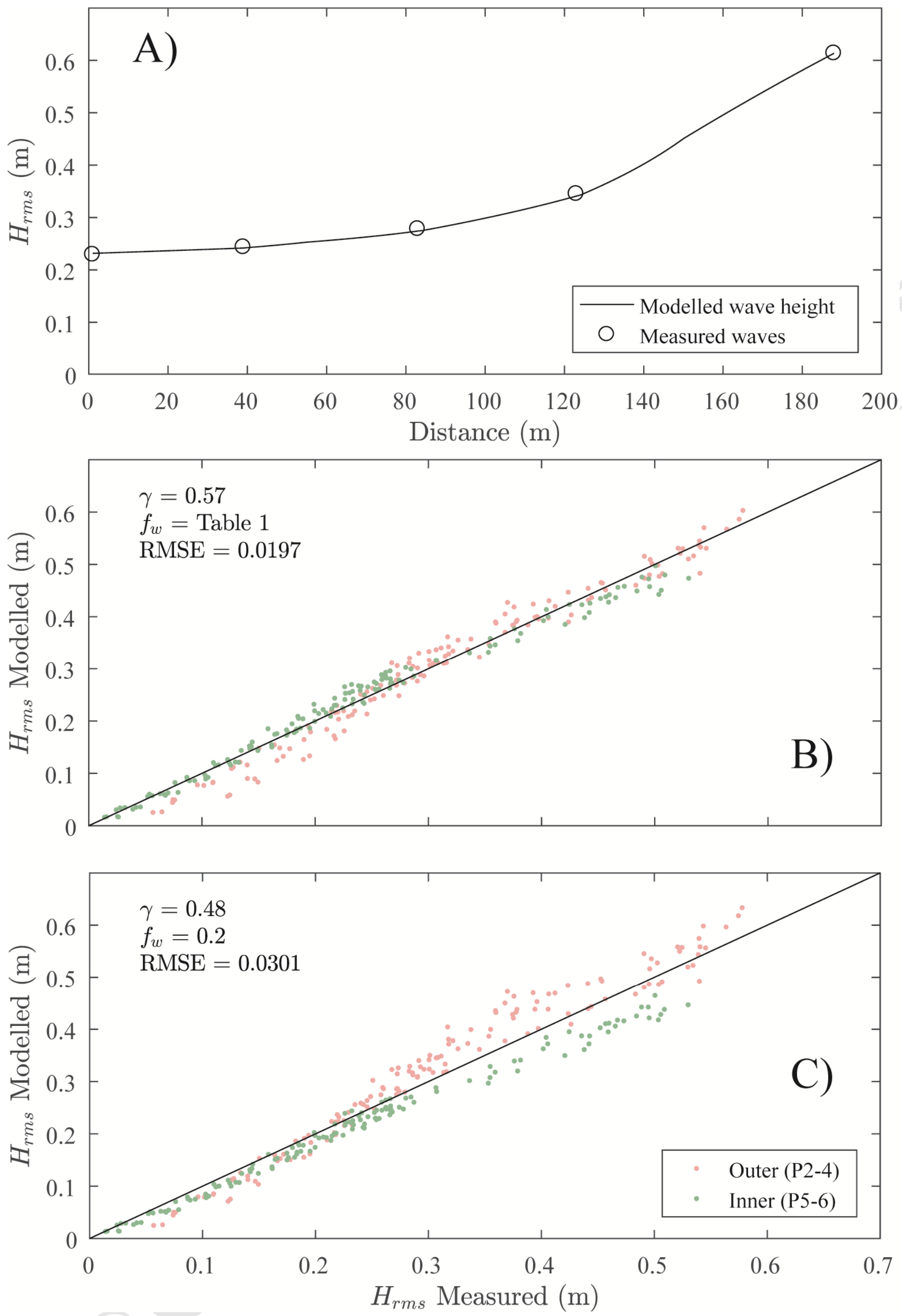

Figure 9. (A) Average cross-reef modelled and measured root-mean-square wave height (H_{rms}); (B) Comparison of measured and modelled waves for the entire deployment record of 2012 with a spatially varying wave friction factor (f_w) shown in Table 1 (see panel (C) for legend); and, (C) a constant f_w value. The inner reef flat is in green and outer reef flat in magenta. The values used for γ and f_w are shown in panels (B) and (C).

Saturated surf zone waves were measured and compared to a common wave energy dissipation model

Surf zone saturation and depth limited wave conditions were observed to vary depending on water depth and location on coral reef flats

Errors were observed in the dissipation model correlated with variation in wave height to water depth ratios in the surf zone

Some errors were corrected by spatially varying bed frictional dissipation on the reef flat

Model calibration from surf zone data is required to accurately describe wave height decay on coral reef flats